



OPEN Pattern reconfigurable quasi Yagi antenna with Origami inspired magic spiral cubes for dynamic indoor IoT applications

Sayed Sabir Shah¹, Slawomir Koziel^{2,3}, Shahid Bashir¹, Eirikur Bernhardtsson², Ahmed Salim⁴ & Syed Imran Hussain Shah⁵✉

This paper presents a novel deployable antenna design with reconfigurable radiation patterns suitable for various indoor Internet of Things (IoT) applications. Inspired by origami, the antenna comprises a central monopole patch housed on a magic cube (MC-2) and two other modular units comprising stacks of magic cubes (MCs). In compact form, i.e., State-1, the antenna occupies a space of 50 mm, whereas in other states, it occupies a maximum of 150 mm space. Pattern reconfigurability is achieved by simply folding or unfolding these units. The antenna operates in four different states. For example, when both MC-1 and MC-3 are folded, the antenna exhibits an omnidirectional pattern (State-1). When either MC-1 or 3 are folded, the antenna shows directional behavior (States 2 and 3), offering $\pm 90^\circ$ beam switching, whereas when both MC-1 and 3 are unfolded, the antenna exhibits bidirectional behavior (State 4), directing the main beam toward 88° and 92° . The antenna operates in the 2 GHz band and exhibits peak gains ranging from 2 dBi to 9 dBi. The excellent agreement between the simulated and measured results validates the design. This cost-effective, reconfigurable antenna presents a promising solution for diverse indoor IoT applications because of its cost-effectiveness and reconfigurable nature.

Keywords Origami antennas, Pattern reconfigurable antennas, Beam switching, Deployable antenna

The exponential growth of wireless communication devices in recent decades has necessitated the development of antennas with increased adaptability. Traditional antennas are restricted by their fixed operating frequencies and radiation patterns, posing a significant challenge for applications that require dynamic characteristics. These applications include radar systems, satellite communications, and mobile networks, IoT networks where adaptable radiation performance is crucial for optimal performance^{1–9}.

Reconfigurability offers a solution by enabling the adjustment of the antenna's key parameters, such as frequency, radiation pattern, and polarization, either individually or in combination. This adaptability enables significant improvements in system performance and potentially reduces the number of antenna elements, leading to more compact and efficient communication system deployment.

The concept of reconfigurable antennas emerged in the 1930s with the introduction of null-steering arrays controlled by phase shifters to determine the signal arrival direction. Subsequent advancements have introduced various reconfigurable techniques, including diodes¹⁰, ferroelectric varactors¹¹, phase shifters, varactor diodes, and microelectromechanical systems (MEMSs)¹². However, these approaches often suffer from limitations such as reduced power handling capability, intricate biasing networks required for component tuning¹³, and potential nonlinear distortions that can compromise signal integrity¹⁴.

Origami technology presents a promising alternative for overcoming these limitations. By exploiting the principles of folding and unfolding origami structures, researchers can create antennas with a diverse range of reconfigurable properties. These pattern reconfigurable antennas can modify their radiation direction at a fixed operating frequency through adjustments in their aperture shape. This capability significantly enhances system performance by enabling the avoidance of noise sources and electronic jamming. Consequently, it leads

¹Department of Electrical Engineering, University of Engineering and Technology, Peshawar, Pakistan. ²Department of Engineering, Reykjavik University, 102 Reykjavik, Iceland. ³Faculty of Electronics, Telecommunication and Informatics, Gdańsk University of Technology, 80-233 Gdańsk, Poland. ⁴Department of Electrical Engineering, Namal University, Mianwali, Pakistan. ⁵School of Electrical and Electronics Engineering, Chung-Ang University, Seoul 06974, Republic of Korea. ✉email: engr.shahsyedimran@gmail.com

to improved system security and energy efficiency through the targeted transmission of signals toward intended users.

The increasing demand for pattern reconfigurable antennas is driven by advancements in modern wireless communication technologies, particularly those employed in satellite communication, radar systems, and military applications^{15–18}. This has spurred research efforts exploring various techniques, encompassing both mechanical and electrical approaches¹⁹, to achieve this functionality. Among these innovative methods, origami-inspired antennas stand out as a particularly promising solution. In these designs, the antenna's radiation pattern is altered by manipulating its physical form through folding and unfolding.

The appeal of origami technology lies in its ability to circumvent the complexities associated with conventional switching mechanisms and their accompanying biasing networks, which can be detrimental to overall system performance. By leveraging the transformation of flat origami patterns into three-dimensional structures, these antennas enable modifications in their radiation patterns through simple folding and unfolding actions. Furthermore, the transition from a 2D configuration to a 3D geometry can induce mode changes, leading to an even wider array of achievable radiation patterns. This design principle has paved the way for the development of a multitude of intriguing pattern reconfigurable origami antenna possibilities.

Pattern reconfigurability is particularly useful in obstacle-dense environments such as urban areas and indoor spaces where it can optimize the signal and direct the beam in a particular direction due to varying propagation conditions. Consequently, this improves the overall performance and dependability of wireless communication systems by enabling stronger signals and more uniform coverage. In addition, the pattern reconfigurable antenna mitigates interference and improves the overall signal-to-noise (SNR) ratio^{20,21}. It allows multiuser communication and enhances network capacity by supporting multiple users with varying spatial distributions with efficient energy usage by steering the beam in the intended direction¹¹. Origami antennas have several advantages over traditional and existing reconfigurable designs. First, they achieve reconfigurability without the need for switches, making them potentially more efficient and reducing power consumption. Second, their compact size allows them to be folded for storage or transport, which is ideal for portable devices. They can then be unfolded and deployed on demand, adding to their versatility. Finally, origami antennas can be reconfigured in real time to adapt to changing signal conditions and optimize performance for different applications. Several studies have explored the potential of origami antennas. For example, the thermally reconfigured antenna design in²² demonstrated both deployability and reconfigurability for an extended mobile range. However, this design involves trade-offs. It offers beamwidth switching and pattern reconfigurability but suffers from a slow actuation speed due to the thermal activation of shape memory polymer (SMP) hinges. The antenna in²³ achieves polarization diversity but is fragile and susceptible to damage. The patch antenna array in²⁴ offers foldability and enhanced beam steering but has a large footprint at 2.4 GHz.

In conclusion, conventional pattern-reconfigurable antennas often rely on active components such as PIN diodes or varactor diodes to achieve reconfigurability. These components can introduce significant losses, limit the achievable reconfiguration range, and necessitate additional power consumption. Moreover, the complex circuitry required to control these components can increase the overall system complexity and cost. In contrast, our proposed origami-based antenna offers a more elegant and efficient solution. By leveraging the principles of origami, we achieve reconfigurability through simple mechanical deformations, eliminating the need for active components and complex circuitry. This results in a more compact, low-cost, lightweight, and power-efficient design.

Our proposed design builds upon the work presented in²⁵, which prioritizes gain enhancement through the addition of directors, creating a quasi-Yagi antenna. However, this design lacks reconfigurability features. Similarly, the DNA-inspired design in²⁶ offers pattern reconfigurability but is limited by a large ground plane, hindering deployment flexibility. By incorporating the advantages of origami and addressing the limitations of existing designs, we aim to develop a new generation of reconfigurable origami antennas that are compact, deployable, and adaptable to meet the demands of modern wireless communication systems.

In this context, we propose a novel origami magic spiral cube-based radiation pattern reconfigurable antenna, inspired by the Yagi geometry. Notably, our antenna is easily deployable on any surface and improves previously reported designs in terms of beam switching capability. The proposed antenna offers remarkable beam control, allowing $\pm 90^\circ$ beam direction switching with a 62° 3 dB beam width for States 2 and 3 or directing its beam by 88° and 92° with corresponding 3 dB beam widths of 51° for State 4, respectively. Our proposed antenna is simpler, more cost-effective, and performs better than the existing designs, which often have thick substrates and large areas. We have simulated and experimentally validated various performance parameters, including impedance bandwidth, directivity, and radiation patterns, on the basis of the fabricated antenna prototype.

In the subsequent sections, we delve into the details of the proposed antenna design, discuss the simulation and measurement results, and conclude by summarizing the main findings and comparisons with state-of-the-art designs reported in the literature.

Antenna design

The proposed antenna consists of three modular elements. One central element having a monopole designed on magic cube2 (MC2) and two parasitic stack elements named MC1 and MC3 which act as a director and reflector alternatively. The complete stepwise design of magic cube from simple plane sheet of paper to final structure is described in Fig. 1 while the different states in which the magic cubes are arranged to perform specified task is illustrated in Fig. 2. Initially two square sheets of paper, S-1 and S-2, each having thickness of 0.65 mm and dimensions of 50 mm × 50 mm were taken (Fig. 1(a)). Both sheets were labeled with reference points (J, J', K, K', L, L', M, M', N, N', O, and Q) to guide the folding process as shown in Fig. 1(b). Sheet S-1 was folded along line JJ' and then unfolded, creating a crease (Fig. 1(c)). The JJ' marking divided the square into two triangular halves (Fig. 1(c)). For the lower triangular half, the sheet was folded along LL' so that point O touched JJ' line

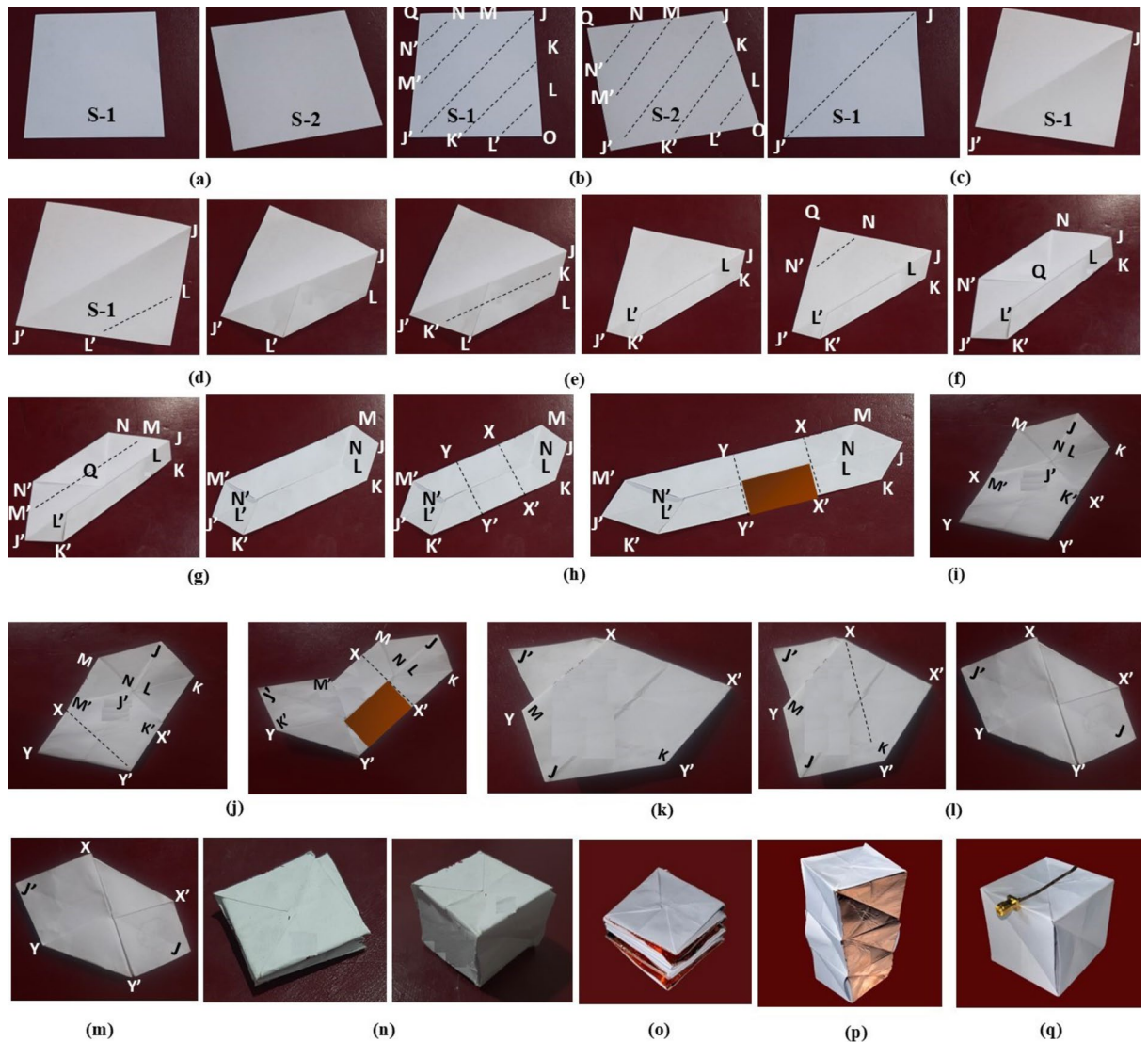


Fig. 1. Step by step design stages of origami magic cube design process for the driven and parasitic elements.

(Fig. 1(d)). Next, it was folded along KK' aligning LL' with JJ' (Fig. 1(e)). Similarly, the upper triangular portion of the sheet was folded along line NN' so that point Q touched line JJ' (Fig. 1(f)). Finally, it was folded along MM' , aligning NN' and LL' with JJ' (Fig. 1(g)). Now for driven magic cube consisting of monopole and ground plane, a 0.1 mm thick copper strip with dimensions $L_g \times L$ was attached to the middle section of sheet S-1 between lines XX' and YY' to act as ground plane of driven monopole (Fig. 1(h)). Sheet S-1 was then folded along YY' so that point J' met points N and L (Fig. 1(i)) so that the hexagonal shape of sheet S-1 was transformed into a pentagon. Now the section $J'K'Y'M'$ was folded towards $YY'M'$ (Fig. 1(j)). The paper was then folded along line XX' (Fig. 1(k)). Finally, section $KJMX$ was folded towards KXX' , resulting in a hexagonal shape again (Fig. 1(l)). Sheet S-2 was folded using the same steps as S-1, excluding the attachment of the copper strip (Fig. 1(m)). The magic cube geometry was then created by joining the folded geometries formed from S-1 and S-2. Figure 1(n) shows that the magic cube has six square sides; each of them has the same dimensions. The magic cube geometry can be conveniently folded and unfolded. After fabricating the magic cube, the monopole driven element was realized on magic cube#2 (MC-2), using copper film (Fig. 1(q)). The parasitic magic cubes #1 and #3 (MC-1 and MC-3) were also fabricated using the same procedure as for MC-1 with copper film completely covering one face of magic cube. The parasitic magic cube design was completed after joining three such magic cubes using a double-sided bonding film. Figure 1(o-p) shows the parasitic magic cube geometry in its folded and unfolded states, respectively.

The proposed antenna leverages three modular origami structures resembling magic cubes (MCs), as shown in Fig. 2. Each module plays a specific role in achieving reconfigurable radiation patterns. The central MC (MC-2) consists of a resonating $\lambda/4$ monopole radiating element. Two parasitic MC (MC-1 and MC-3), each consisting of three stacked conducting surfaces, are adjacent to MC-2 on either side. These parasitic elements function as directors, focusing radiation on them when their electrical length is less than $\lambda/4$. Conversely, they

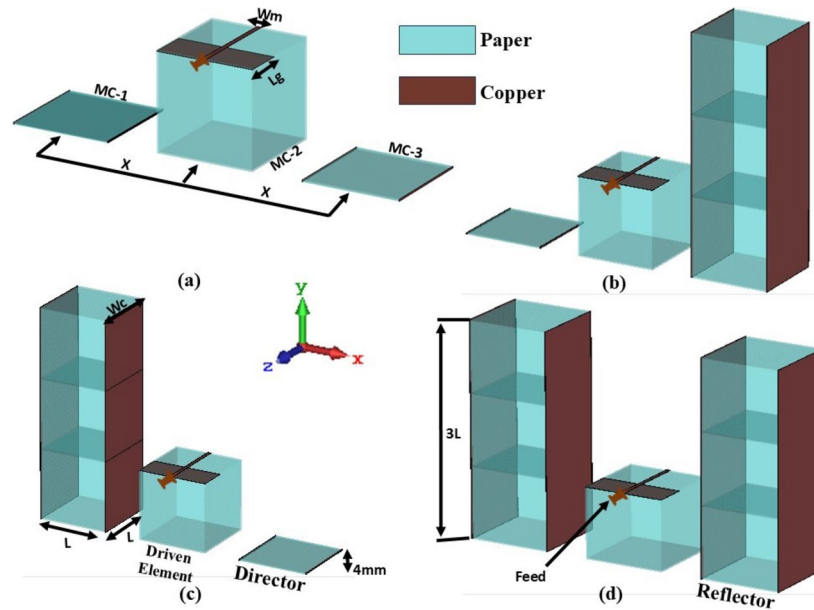


Fig. 2. Proposed deployable origami pattern reconfigurable antenna design for various state arrangements with $L = WC = 50$ mm, $L_g = 20$ mm, $W_m = 2.5$ mm, $X = 76$ mm (a) State-1 (b) State-2 (c) State-3 (d) State-4.

act as reflectors, redirecting radiation away from themselves when their electrical length exceeds $\lambda/4$. By simply folding or unfolding these elements, we can modify their electrical lengths and adjust the antenna's radiation pattern to achieve the desired directionality.

The driven monopole radiator in MC-2 consists of a copper strip with length $L = 0.3\lambda$ and width $W_m = 0.016\lambda$ attached to the top surface. Its ground plane with $L_g = 0.13\lambda$ is integrated on the interior of MC-2, where $\lambda = 150$ mm at 2 GHz. Similarly, parasitic elements MC-1 and MC-3 employ conducting surfaces on two sides.

The proposed design uses a standard 0.65 mm thick, 50 mm \times 50 mm paper sheet for structural support. The conductor elements are made from 0.1 mm thick copper tape with a conductivity of 4.4×10^5 S/m²⁵.

By manipulating these MCs through folding and unfolding, we achieve four distinct radiation patterns, as illustrated in Fig. 2:

- State-1 (Fig. 2(a)): Both MC-1 and MC-3 are folded, acting as directors in a configuration similar to a Yagi antenna. They minimally affect radiation, resulting in an omnidirectional pattern from the driven element (monopole antenna) in MC-2.
- State-2 (Fig. 2(b)): MC-1 remain folded (director), whereas MC-3 unfold (reflector). This configuration directs radiation away from the reflector side.
- State-3 (Fig. 2(c)): MC-3 is folded (director), and MC-1 unfolds (reflector). The radiation pattern is similar to that of State-2 but in the opposite direction.
- State-4 (Fig. 2(d)): Both MC-1 and MC-3 are unfolded (reflectors). Compared with other states, the radiation pattern becomes bidirectional, with a slight decrease in bandwidth and a gain enhancement of 1 dB.

Figure 3(a) shows the fabricated prototype demonstrating the folding/unfolding mechanism of origami magic cube structure for reconfigurable states. As can be seen the parasitic magic cube structure consisting of 3 magic cubes in stack configuration can be manually folded/unfolded in 3 steps. The feed magic cube consisting of single magic cube remains in unfolded configuration for all operating states. The testing of fabricated model has been conducted in an anechoic chamber with setup shown in Fig. 3(b).

Figure 4 shows the fabricated prototype operating in four reconfigurable states. Figure 4(a) shows state 1 configuration where both parasitic MC are folded. Figure 4(b) shows state 2 configuration where the left parasitic MC is folded while right parasitic MC is unfolded. Similarly Fig. 4(c) shows state 3 configuration where left parasitic MC is unfolded while right parasitic MC is folded. Figure 4(d) shows the proposed model in state 4 configuration where both left, and right parasitic MCs are unfolded.

Parametric analysis

A comprehensive parametric study was conducted to optimize the performance and size of the proposed antenna design. We first investigated the impact of the design parameters on the antenna's reflection coefficient. The paper substrate thickness T_s was varied from 0.1 mm to 0.7 mm, and a thickness of 0.65 mm was found to be optimal for achieving good impedance matching at an operating frequency of 2 GHz (Fig. 5(a)).

Similarly, varying the interelement spacing X between the central and side elements (from 50 mm to 85 mm) led to an optimal value of 76 mm (Fig. 5(b)). Additionally, the effect of the copper sheet width W_c on impedance matching was also studied, as shown in Fig. 5(c).

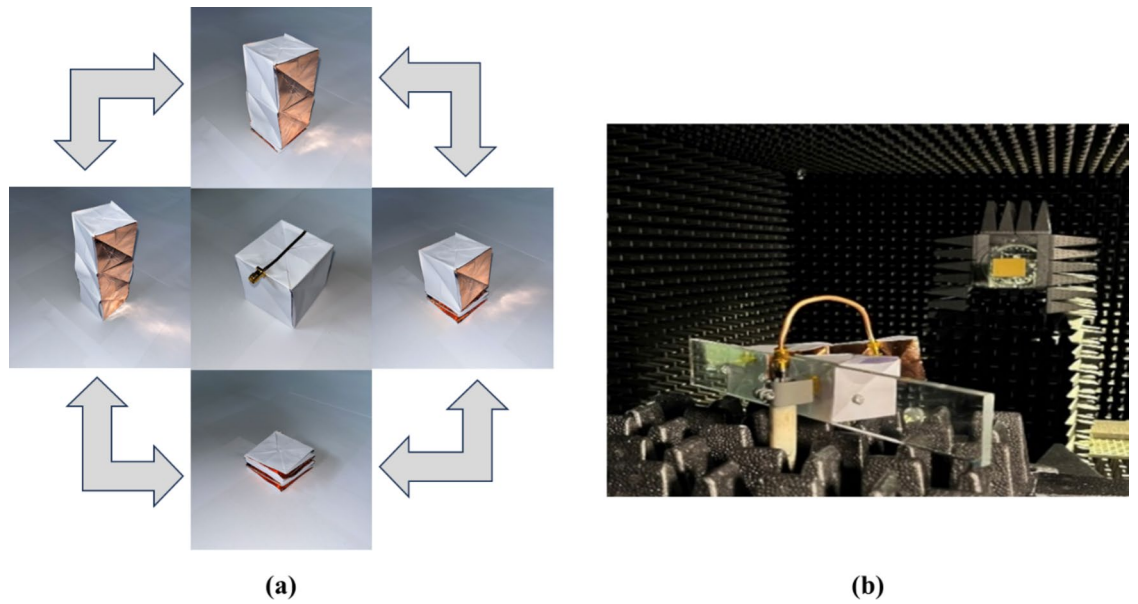


Fig. 3. Fabricated Magic Cube structure (a) Magic Cube folding/unfolding stages (b) Measurement setup.

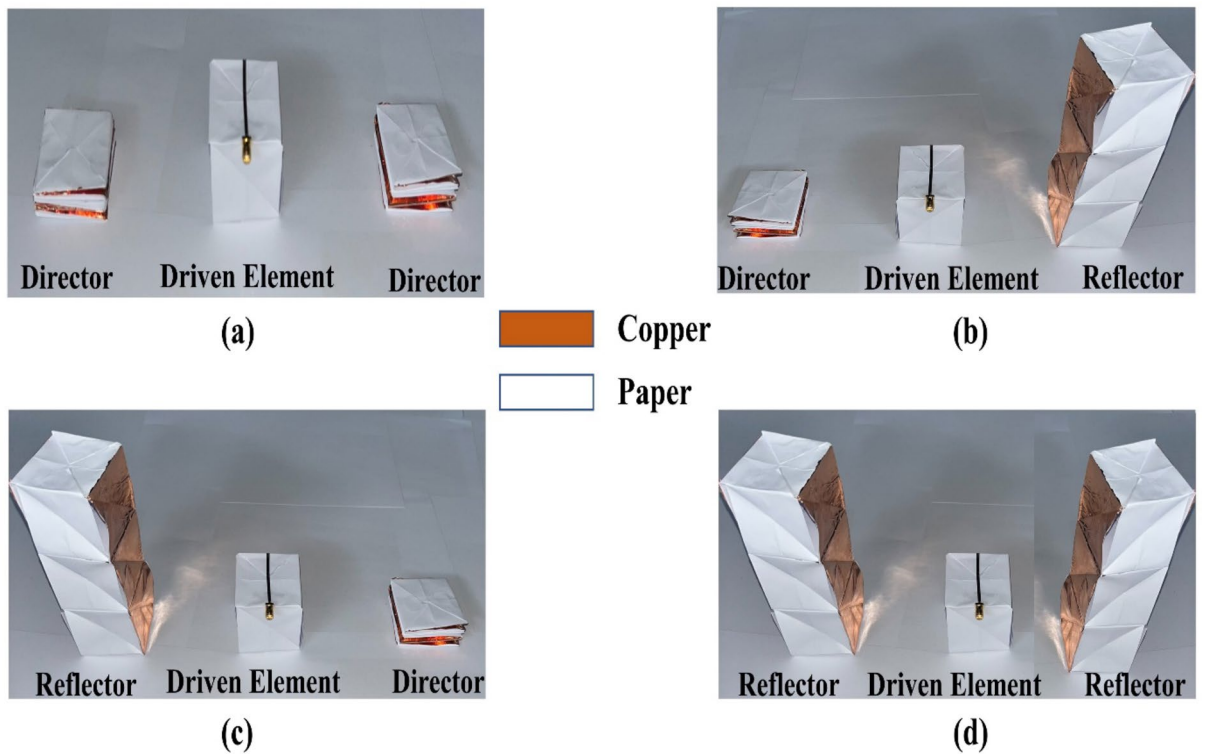


Fig. 4. Fabricated prototypes in different state configurations : (a) State-1 (b) State-2 (c) State-3 (d) State-4.

Next, we analyzed the effect of the copper sheet width W_C on the gain (Fig. 6(a)). The maximum gain was achieved for $W_C = 50$ mm, whereas the minimum gain was observed for $W_C = 5$ mm. A gain variation of almost 1 dB for every 5 mm change in W_C for all four states (1, 2, 3, 4) of the design can be observed. To achieve an optimal balance between size and performance, the effect of the number of magic cubes on the gain for all states was studied. Figure 6(b) shows that three stacked magic cubes provide the highest gain.

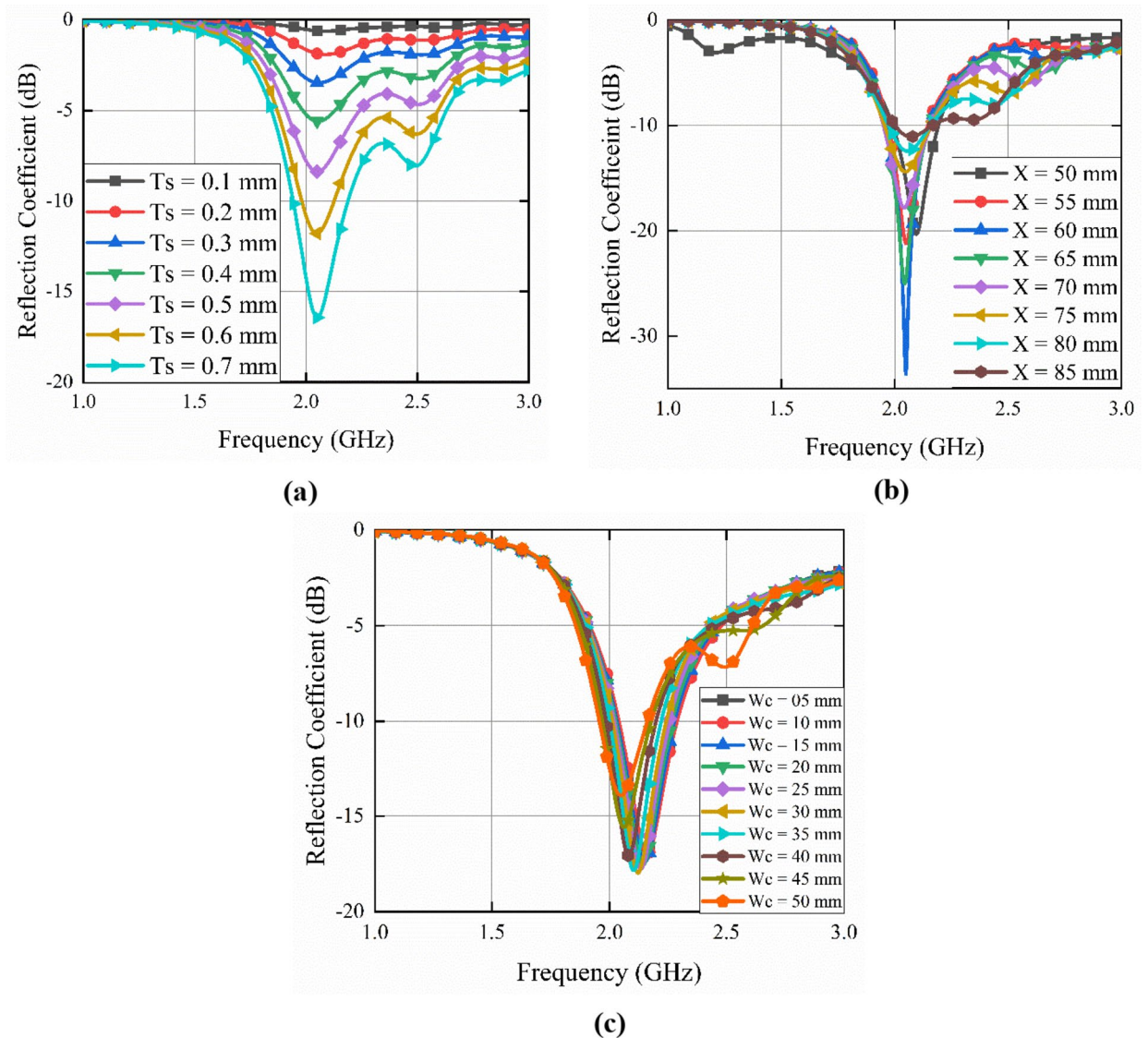


Fig. 5. Reflection coefficient of the proposed antenna (a) variation with substrate thickness (T_s), (b) variation with interelement spacing (X) between magic cubes and (c) variation with copper width (W_c).

Results and discussion

The surface current distribution of the proposed antenna, as shown in Fig. 7, plays a critical role in determining its radiation pattern. This is evident across the four distinct states.

In State 1 (Fig. 7(a)), the current distribution is concentrated primarily on the monopole radiator located on MC-2. This results in an omnidirectional radiation pattern, meaning that the antenna emits signals with equal strength in all directions. Notably, the minimal current on MC-1 and MC-3 is in this state.

State 2 (Fig. 7(b)) introduces a change. Current excitation extends from the main monopole radiator on MC-2 to the left-side element, MC-3. This additional current causes MC-3 to act as a reflector, pushing the maximum radiation pattern toward the left side in the direction of MC-2.

State 3 (Fig. 7(c)) shares similarities with State 2 in terms of current flow on the main monopole radiator (MC-2). However, in this state, current is present on the right-side element, MC-1, rather than MC-3. Consequently, the omnidirectional pattern observed in State 1 transforms into a directional pattern with the maximum radiation pushed toward the right side in the direction of MC-3.

Finally, in State 4 (Fig. 7(d)), the current is excited on all three elements: the main monopole radiator (MC-2) and both parasitic elements (MC-1 and MC-3). This configuration enhances radiation in opposite directions from MC-1 and MC-3, leading to a bidirectional radiation pattern.

The proposed antenna exhibits different radiation patterns depending on the folding configuration of the parasitic elements (directors/reflectors). The 3D radiation patterns shown in Fig. 8 further illustrate how configuration choices influence performance. With folded parasitic elements (State-1), the antenna exhibits an omnidirectional pattern (Fig. 8(a)). The pattern becomes directional with changes in the main lobe direction when either one or both parasitic magic cubes are unfolded (Fig. 8(b-d)). State-1 shows a gain of 3.41 dBi and an

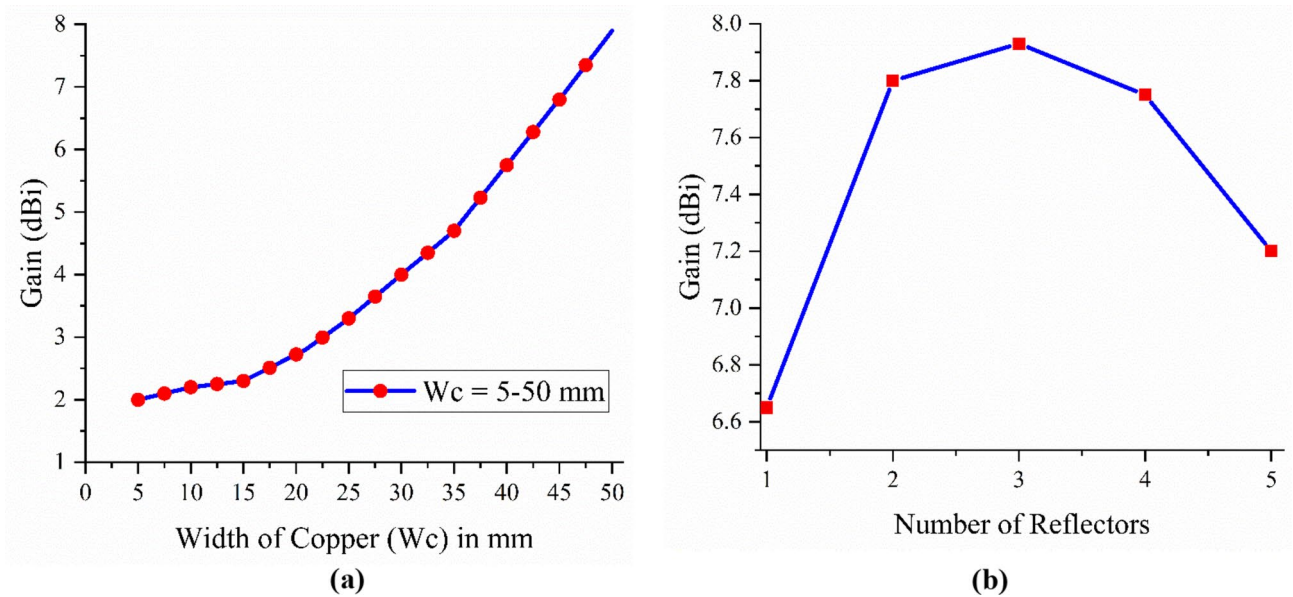


Fig. 6. (a) Effect of the copper width (W_c) on the gain of the proposed antenna. (b) Effect of the number of magic cubes (MC-1 and MC-2 when used as reflectors) on the gain of the proposed antenna.

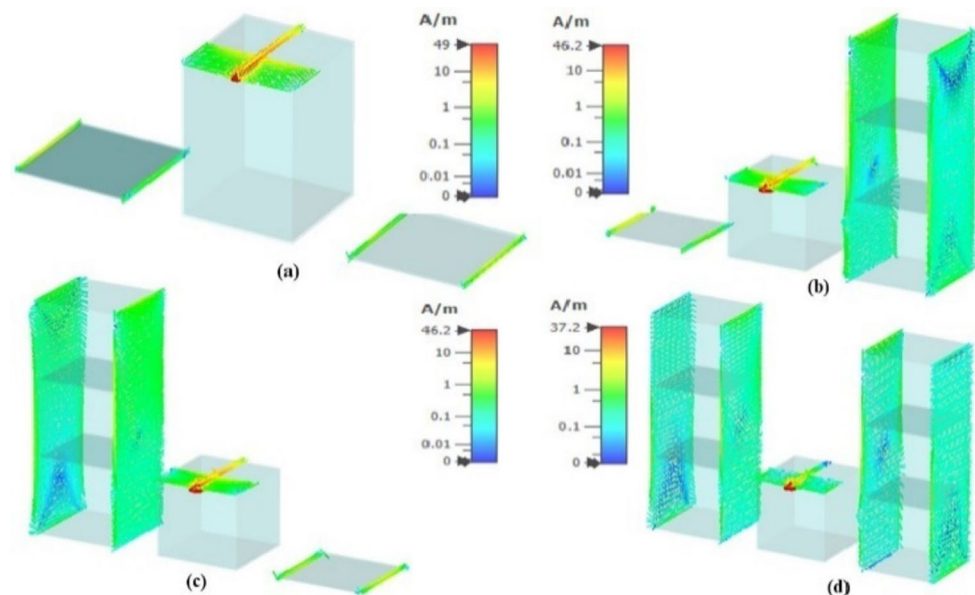


Fig. 7. Surface current distributions for various states, i.e., (a) State-1 (b) State-2 (c) State-3 (d) State-4.

omnidirectional pattern. Likewise, in State-2, the antenna exhibits a gain of 7.94 dBi, and the main lobe points to 90° with a 3 dB beam width of 62° . Figure 8(c) illustrates state 3, which is similar to State-2 except for the direction of maximum radiation in the opposite direction. Finally, in State-4, the antenna shows bidirectional behavior and a gain of 9.07 dBi, and the main lobe points toward 88° and 92° , with a 3 dB beamwidth recorded as 51° .

Figure 9(a) compares the simulated and measured reflection coefficients for State-1, where both parasitic elements act as directors. The slight frequency shift and reduced antenna size due to the folded elements are evident. Figure 9(b) and 9(c) compare the results for States 2 and 3, where the parasitic elements act as directors and reflectors alternatively. State-3 has a similar pattern to State-2, with the main radiation direction flipped due to the swapped configuration. Figure 9(d) shows the reflection coefficient for State-4, where both elements act as reflectors. The slight left shift is due to the increased size of the antenna with unfolded elements. We designed the antenna to operate at 2 GHz however as the main radiating structure is a resonating element it can be easily scaled to any frequency band by changing its electrical length or by using some other origami substrate like

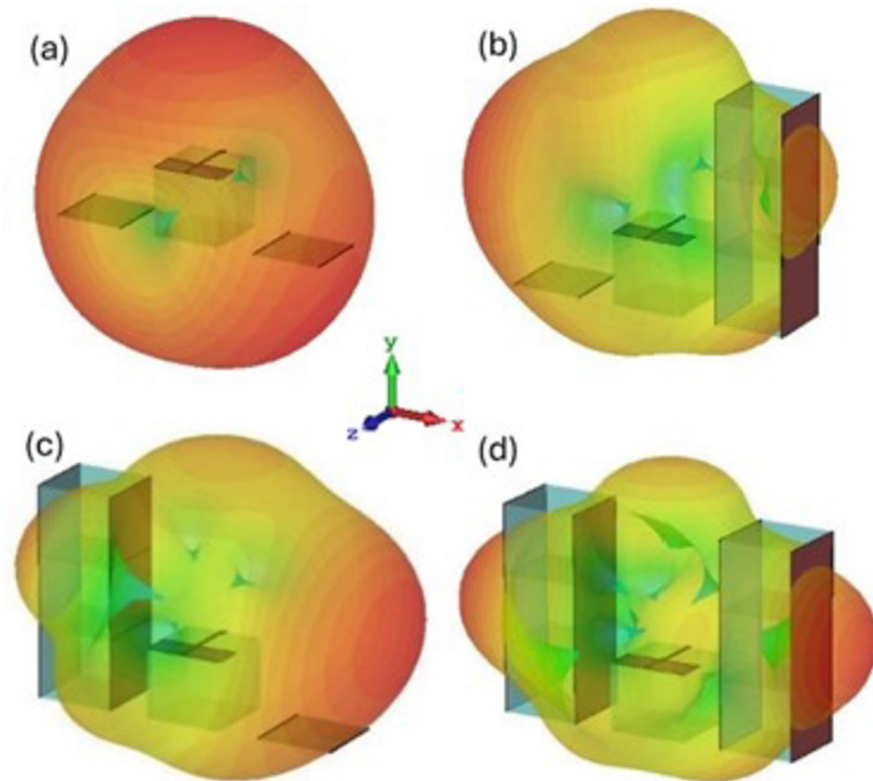


Fig. 8. 3D radiation pattern of the proposed design for four different states: (a) State 1, (b) State 2, (c) State 3, and (d) State 4.

Polyethylene terephthalate (PET). For adapting the design to higher frequencies than 2 GHz the overall antenna size will decrease whereas its overall size will increase for lower frequency applications.

The normalized simulated and measured radiation patterns in the E-plane (similar for all states and showing donut-shaped behavior) are presented in Fig. 10.

The normalized simulated and measured radiation patterns in the H-plane are presented in Fig. 11. State-1 exhibits omnidirectional behavior, whereas States-2 and 3 show directional behavior with beam switching capabilities of $\pm 90^\circ$ and a 3 dB beam width of 62° . Finally, State-4 exhibits a bidirectional pattern with the main lobe at 88° and 92° and a 3 dB beam width of 51° . The final optimized variables with their optimum values are summarized in Table I.

Table 2 compares our proposed design with other reconfigurable antenna design types. Our proposed design offers several advantages over existing origami-based reconfigurable antenna designs. In²⁷, the antenna height changes in frequency, but its large size ($100\text{ mm} \times 100\text{ mm}$ base, 273 mm height) hinders deployment in certain applications. Similarly, the SMP hinge antenna in²² offers good gain at moderate cost; it requires a hot plate for actuation, limiting its practicality. The design in²⁵ lacks reconfigurability but achieves compactness and improved directivity solely through actuation. The DNA-inspired antenna in²⁶ offers optimal gain, but its square substrate restricts its use on curved surfaces. The conical spiral antenna in²⁸ achieves frequency and polarization reconfiguration, but its planar stage dimensions and intricate fabrication steps pose challenges. In contrast, our proposed design stands out for its simplicity, low cost, and significantly high gain, making it a compelling choice for diverse conformal and IoT applications.

Conclusion

This work introduces a versatile, deployable pattern-reconfigurable origami antenna capable of switching its radiation pattern across four distinct states. It can be easily folded and unfolded, making it ideal for portable and space-constrained applications. The proposed antenna is cost-effective as readily available copper tape is used as the conductor part, and standard print paper is employed as the substrate part of the antenna. The origami-inspired design allows for rapid deployment, saving time and effort. The antenna's radiation pattern can be dynamically adjusted to optimize performance for different scenarios. The proposed antenna can steer its beam to different intended locations by just folding the mechanism.

The innovative origami magic cube design, which is fabricated from a simple sheet of paper and copper tape by simple folding or unfolding, can direct its beam between $\pm 90^\circ$ with a 62° 3 dB beam width in State-2 and State-3 and demonstrate a bidirectional pattern by pointing its beam at 88° and 92° with a 3 dB beam width of 51° , respectively. It achieves a maximum gain of 9 dBi with an impedance bandwidth of 10.5%. These features



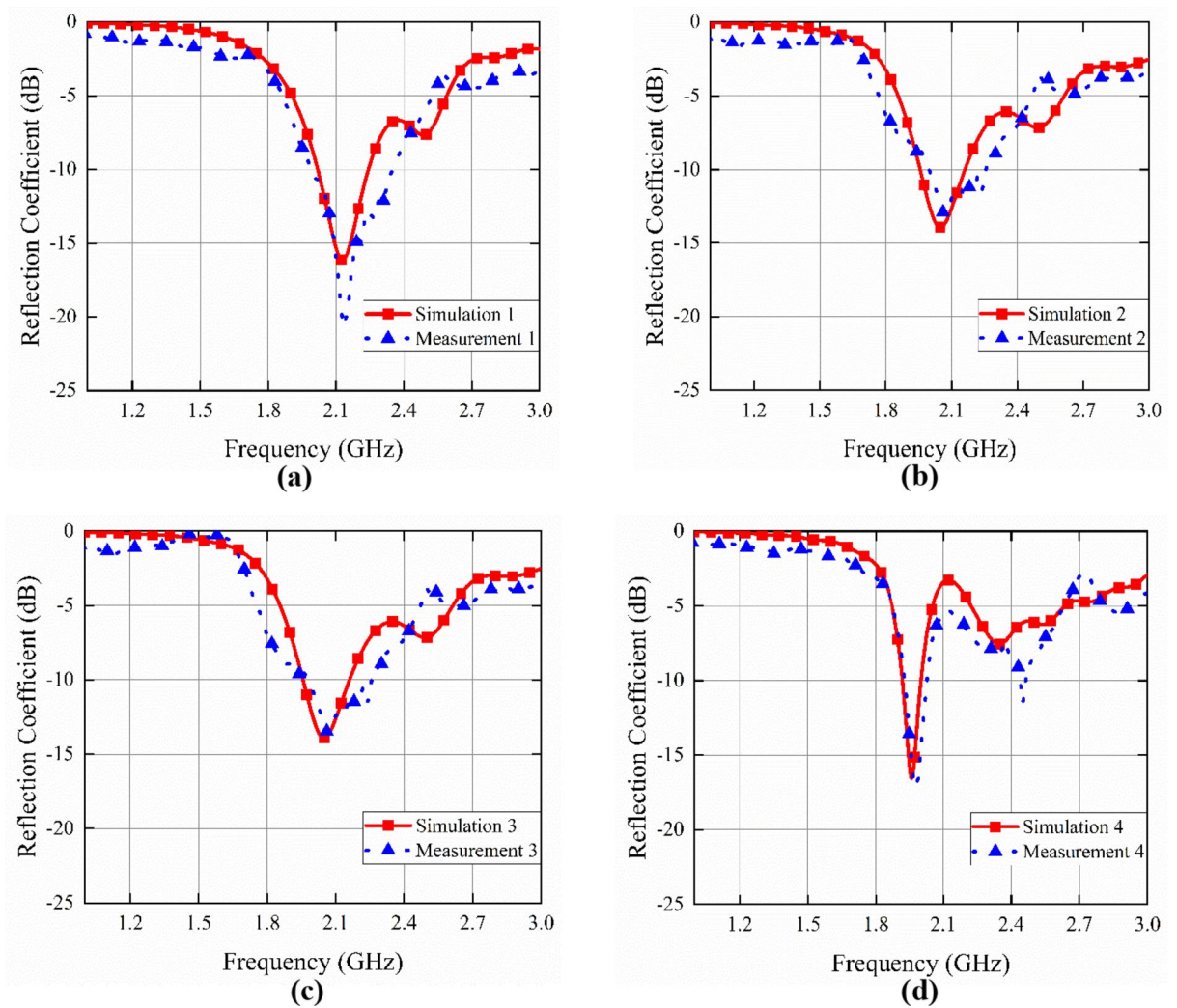


Fig. 9. Simulated and measured reflection coefficients for different states: (a) State 1 (b) State 2 (c) State 3 (d) State 4.

are combined to create a compact, deployable antenna solution with remarkable adaptability for diverse wireless communication needs.

Beyond its cost-effectiveness, the simplicity and reconfigurability inherent in origami-based designs hold the potential to revolutionize wireless technology. Specifically, this antenna's ability to reconfigure its radiation pattern direction is a valuable tool for a range of indoor applications. In environments such as warehouses and factories, it can facilitate real-time equipment tracking and movement monitoring. This is just a glimpse into the vast potential of this reconfigurable antenna and its impact on the future of indoor wireless communication.

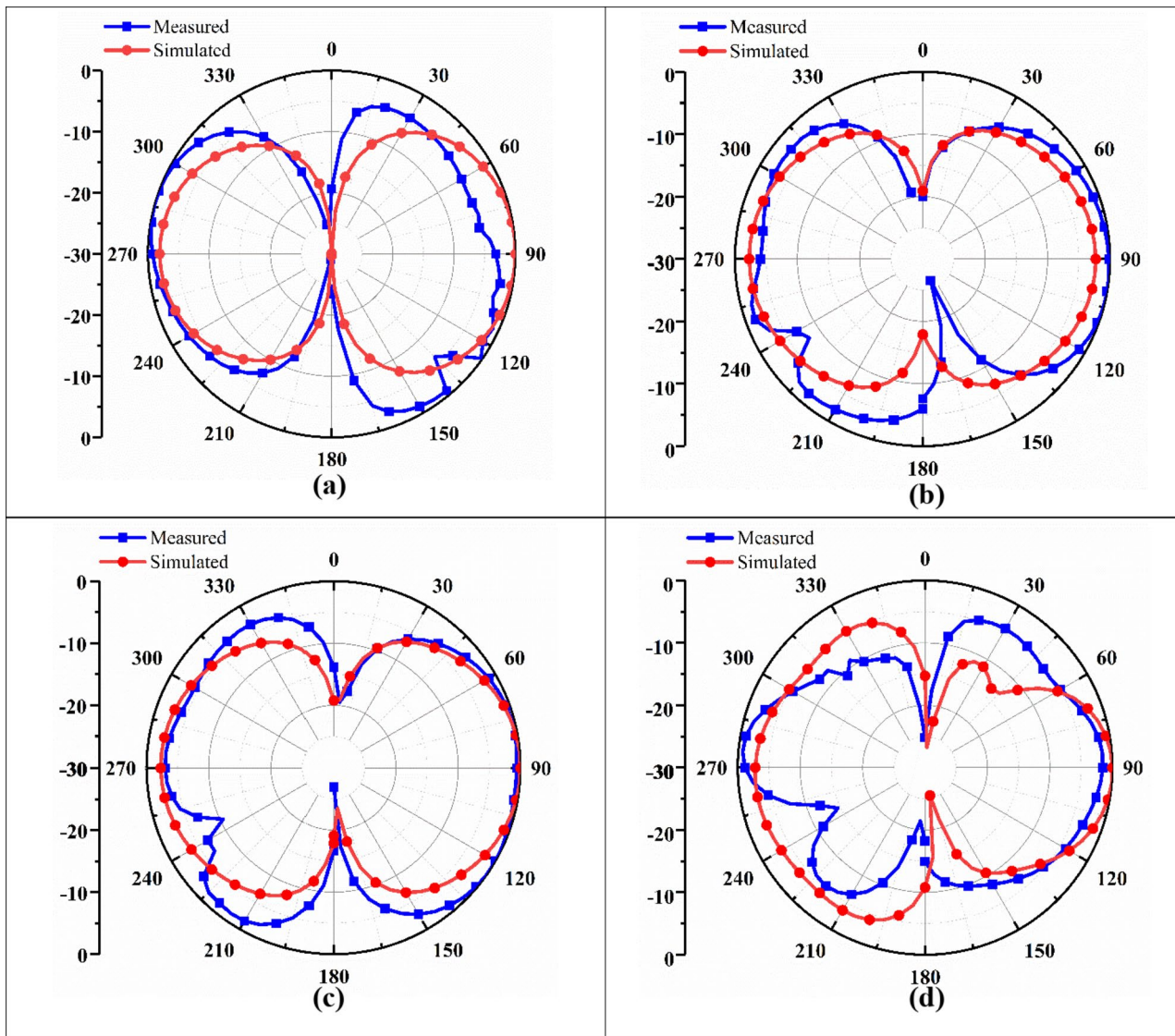


Fig. 10. Simulated and measured normalized radiation patterns in the E-Plane for different States: (a) State 1 (b) State 2 (c) State 3 (d) and State 4.

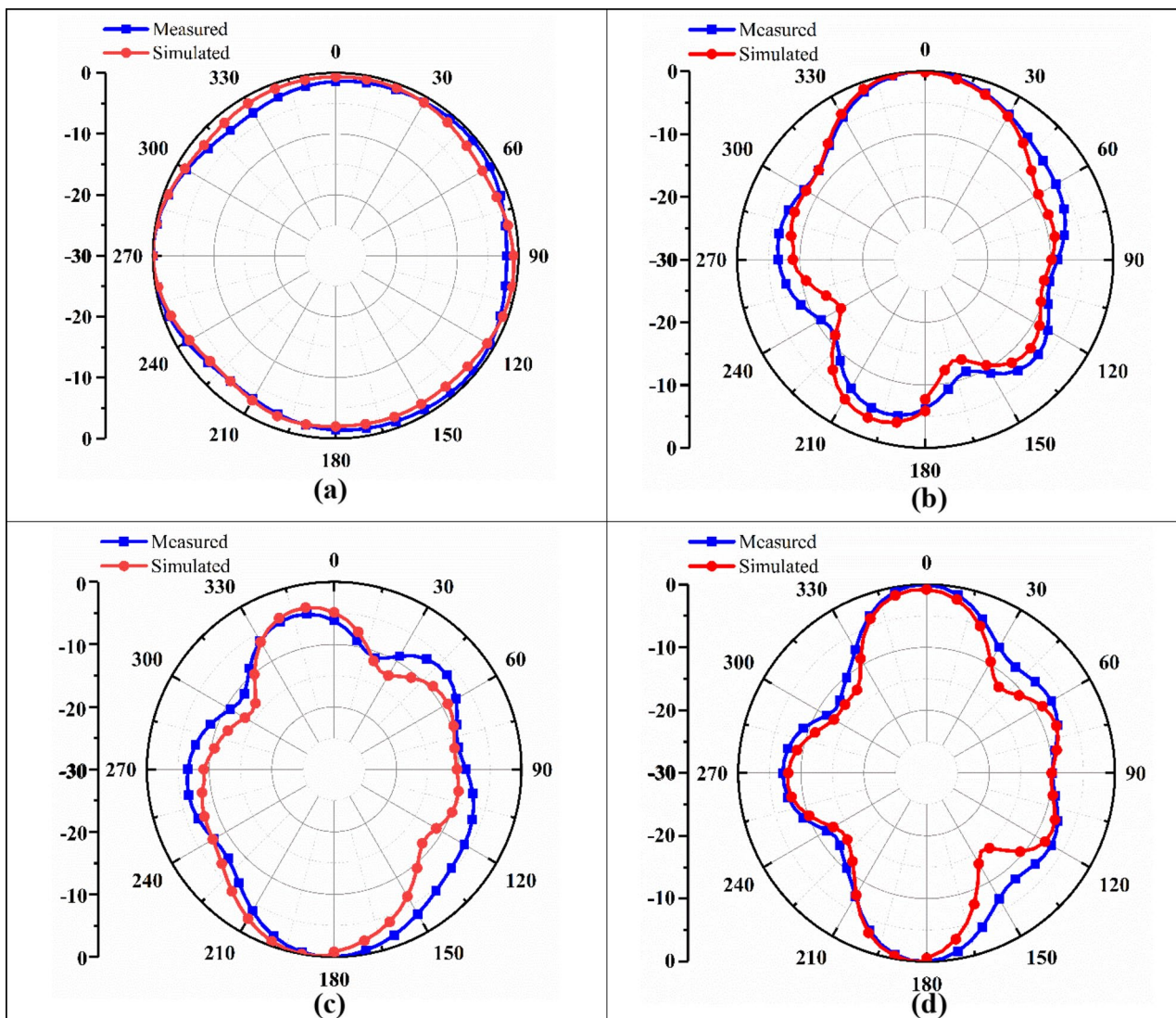


Fig. 11. Simulated and measured normalized radiation patterns in the H-Plane for different States: (a) State 1 (b) State 2 (c) State 3 (d) and State 4.

Symbol	Quantity	Value (mm)
Ts	Thickness of Sheet	0.65
X	Inter element (MCs) Spacing center to center	76
WC	Metallic strip width	50

Table 1. Optimization of the antenna parameters.

Ref.	Antenna Type	Reconfiguration	Switching Mechanism	Peak Gain (dBi)	BW (%)	Radiation efficiency (%)	Substrate	Antenna Design	Cost
22	Monopole	Pattern	Thermal	11	18	NA	FR-4	Complex	High
25	Monopole	Nil	Mechanical	7.3	3.5	NA	Paper	Simple	Low
26	Monopole	Pattern	Mechanical	5.5	7	64	Paper	Moderate	Low
27	Helical	Frequency	Mechanical	6.7	5	NA	Paper	Moderate	Low
28	Patch Dipole	Compound	Mechanical	8.5	1.78	NA	Rogers	Complex	High
This work	Monopole	Pattern	Mechanical	9	10	96	Paper	Simple	Low

Table 2. Comparison with state-of-the-art methods.

Data availability

The data that support the findings of this study are available upon reasonable request from the corresponding author at the email: engr.shahsyedimran@gmail.com.

Received: 21 October 2024; Accepted: 10 March 2025

Published online: 23 March 2025

References

- Cui, Y., Nauroze, S. A., Bahr, R. & Tentzeris, M. M. A novel additively 4D printed Origami-inspired tunable Multi-layer frequency selective surface for mm-Wave IoT, RFID, WSN, 5G, and smart City applications. *IEEE MTT-S Int. Microw. Symp. Digest.* **2021-June**, 86–89 (2021).
- Zhang, Y., Li, M., Chen, Y., Peng, R. & Zhang, X. Thick-panel origami-based parabolic cylindrical antenna. *Mech. Mach. Theory.* **182**, 105233 (2023).
- Jamal, H., Al, Hu, C., Kwao, E., Zeng, K. & Tentzeris, M. M. Toward 5G/mm-Wave Shape-Changing Origami-Inspired phased arrays for Near-Limitless arbitrarily reconfigurable radiation patterns: realization, actuation, and calibration. *IEEE Trans. Microw. Theory Tech.* <https://doi.org/10.1109/TMTT.2024.3463484> (2024).
- Yao, S., Zekios, C. L. & Georgakopoulos, S. V. A rigidly foldable and reconfigurable Thick Origami antenna. *Philosophical Trans. A* **382**, (2024).
- Mishra, A. K. et al. Robotic antennas using liquid metal Origami. *Adv. Intell. Syst.* **6**, 2400190 (2024).
- Russo, A. et al. Origami-inspired self-deployable reflectarray antenna. *Acta Astronaut.* **213**, 240–251 (2023).
- Bichara, R. M., Costantine, J., Tawk, Y. & Sakovsky, M. A multi-stable deployable quadrifilar helix antenna with radiation reconfigurability for disaster-prone areas. *Nature Communications* **2023** 14:1 14, 1–12 (2023).
- Soto-Valle, G., Hu, K., Holda, M., Cui, Y. & Tentzeris, M. Novel additive Manufacturing-Enabled RF devices for 5G/mmWave, IoT, smart skins, and wireless sensing applications. (2022). <https://doi.org/10.1142/S0129156422400171> 31.
- Georgakopoulos, S. V. et al. Origami antennas. *IEEE Open. J. Antennas Propag.* **2**, 1020–1043 (2021).
- Gu, C. et al. Compact smart antenna with electronic Beam-Switching and reconfigurable polarizations. *IEEE Trans. Antennas Propag.* **63**, 5325–5333 (2015).
- Jiang, H. et al. Miniaturized and reconfigurable CPW square-ring slot antenna loaded with ferroelectric BST thin film varactors. *IEEE Trans. Antennas Propag.* **60**, 3111–3119 (2012).
- Kim, I. & Rahmat-Samii, Y. RF MEMS switchable slot patch antenna integrated with bias network. *IEEE Trans. Antennas Propag.* **59**, 4811–4815 (2011).
- Bai, X., Su, M., Liu, Y. & Wu, Y. Wideband Pattern-Reconfigurable cone antenna employing Liquid-Metal reflectors. *IEEE Antennas Wirel. Propag. Lett.* **17**, 916–919 (2018).
- Li, M. & Behdad, N. Fluidically tunable frequency selective/phase shifting surfaces for high-power microwave applications. *IEEE Trans. Antennas Propag.* **60**, 2748–2759 (2012).
- Nikolaou, S. et al. Pattern and frequency reconfigurable annular slot antenna using pin diodes. *IEEE Trans. Antennas Propag.* **54**, 439–448 (2006).
- Utayo, M., Sangthongngam, W., Kittiyapunya, C. & Krairiksh, M. Pattern and frequency reconfigurable meander line Yagi-Uda antenna. *Int. Conf. Adv. Technol. Commun.* **2016-January**, 56–58 (2016).
- Wang, Y. et al. Packing optimization and design of the deployable parabolic rigid antenna based on Origami. *Adv. Space Res.* **73**, 6226–6240 (2024).
- Tian, D. et al. Design and analysis of a solid surface deployable antenna mechanism based on flasher rigid Origami. *Thin-Walled Struct.* **201**, 112033 (2024).
- Ali, M. & Wahid, A. A reconfigurable Yagi array for wireless applications. *IEEE Antennas Propag. Soc. AP-S Int. Symp. (Digest)*, **1**, 466–467 (2002).
- Qin, P. Y., Guo, Y. J., Weily, A. R. & Liang, C. H. A pattern reconfigurable U-slot antenna and its applications in MIMO systems. *IEEE Trans. Antennas Propag.* **60**, 516–528 (2012).
- Li, P. K., Shao, Z. H., Wang, Q. & Cheng, Y. J. Frequency- and pattern-reconfigurable antenna for multistandard wireless applications. *IEEE Antennas Wirel. Propag. Lett.* **14**, 333–336 (2015).
- Shah, S. I. H. & Lim, S. Thermally Beam-Direction- and Beamwidth-Switchable monopole antenna using Origami reflectors with smart shape memory polymer hinges. *IEEE Antennas Wirel. Propag. Lett.* **18**, 1696–1700 (2019).
- Yao, S. & Georgakopoulos, S. V. Origami segmented helical antenna with switchable sense of polarization. *IEEE Access.* **6**, 4528–4536 (2017).
- Hamza, M., Zekios, C. L. & Georgakopoulos, S. V. A Thick Origami reconfigurable and packable patch array with enhanced beam steering. *IEEE Trans. Antennas Propag.* **68**, 3653–3663 (2020).
- Shah, S. I. H., Tentzeris, M. M. & Lim, S. A. Deployable Quasi-Yagi monopole antenna using three Origami magic spiral cubes. *IEEE Antennas Wirel. Propag. Lett.* **18**, 147–151 (2019).
- Shah, S. I. H., Lim, S. & Bioinspired, D. N. A. Origami Quasi-Yagi Helical Antenna with Beam Direction and Beamwidth Switching Capability. *Scientific Reports* **2019** 9:1 9, 1–9 (2019).
- Liu, X., Yao, S., Cook, B. S., Tentzeris, M. M. & Georgakopoulos, S. V. An Origami reconfigurable Axial-Mode bifilar helical antenna. *IEEE Trans. Antennas Propag.* **63**, 5897–5903 (2015).
- Yao, S., Liu, X. & Georgakopoulos, S. V. Morphing Origami conical spiral antenna based on the Nojima wrap. *IEEE Trans. Antennas Propag.* **65**, 2222–2232 (2017).

Acknowledgements

This work was supported in part by the Icelandic Research Fund under Grant 2410297 and in part by the National Science Centre of Poland under Grant 2022/47/B/ST7/00072.

Author contributions

S.S.S. conducted the simulations, developed the methodology, investigated the topic, and wrote the initial draft of the manuscript. S.K. secured funding for the research, supervised the project, and conducted formal analysis. S.B. curated and validated the data, supervised the project, and reviewed and edited the manuscript. E.B. provided the measurement data. A.S. conducted formal analysis and supervised the project. S.I.H.S. conceptualized the research, supervised the project, and reviewed and edited the manuscript.

Declarations

Competing interests

The authors declare no competing interests.

Additional information

Correspondence and requests for materials should be addressed to S.I.H.S.

Reprints and permissions information is available at www.nature.com/reprints.

Publisher's note Springer Nature remains neutral with regard to jurisdictional claims in published maps and institutional affiliations.

Open Access This article is licensed under a Creative Commons Attribution-NonCommercial-NoDerivatives 4.0 International License, which permits any non-commercial use, sharing, distribution and reproduction in any medium or format, as long as you give appropriate credit to the original author(s) and the source, provide a link to the Creative Commons licence, and indicate if you modified the licensed material. You do not have permission under this licence to share adapted material derived from this article or parts of it. The images or other third party material in this article are included in the article's Creative Commons licence, unless indicated otherwise in a credit line to the material. If material is not included in the article's Creative Commons licence and your intended use is not permitted by statutory regulation or exceeds the permitted use, you will need to obtain permission directly from the copyright holder. To view a copy of this licence, visit <http://creativecommons.org/licenses/by-nc-nd/4.0/>.

© The Author(s) 2025